
DYNAMIC DEEP-REINFORCEMENT-LEARNING ALGORITHM IN PARTIALLY OBSERVED MARKOV DECISION PROCESSES *

Saki Omi, Hyo-Sang Shin, Namhoon Cho, Antonios Tsourdos
The School of Aerospace, Transport and Manufacturing
Cranfield University
Cranfield, U.K.
{s.omi, h.shin, n.cho, a.tsourdos}@cranfield.ac.uk

ABSTRACT

Reinforcement learning has been greatly improved in recent studies and an increased interest in real-world implementation has emerged in recent years. In many cases, due to the non-static disturbances, it becomes challenging for the agent to keep the performance. The disturbance results in the environment called Partially Observable Markov Decision Process. In common practice, Partially Observable Markov Decision Process is handled by introducing an additional estimator, or Recurrent Neural Network is utilized in the context of reinforcement learning. Both of the cases require to process sequential information on the trajectory. However, there are only a few studies investigating the effect of information to consider and the network structure to handle them. This study shows the benefit of action sequence inclusion in order to solve Partially Observable Markov Decision Process. Several structures and approaches are proposed to extend one of the latest deep reinforcement learning algorithms with LSTM networks. The developed algorithms showed enhanced robustness of controller performance against different types of external disturbances that are added to observation.

Keywords TD3 · Recurrent neural network · POMDP · robustness · causality

1 Introduction

Machine learning (ML) techniques are widely applied for control tasks. Data-driven approach aided by ML algorithms could be beneficial since it does not necessarily require a system model. More specifically, recent developments in deep reinforcement learning (RL) techniques have been adapted to generate near-optimal actions in the given state of the agent in the continuous action and state space. The latest development of deep RL has been successfully tested in many complex simulation environments from the standardized framework in Open AI gym [1].

However, it is not guaranteed that the RL algorithm showing good performance in the simulation environment will perform as intended in the real world. Although most of the RL algorithms have been built upon the assumption of the Markov Decision Process (MDP), this assumption is not valid in many real-world applications. The information collected from the sensors does not fully describe the true and full state of the agent due to the limited measurement, noise, and disturbances. This partially observable and non-deterministic scenario is categorized as Partially Observable Markov Decision Process (POMDP) [2]. In the MDP condition, it is possible to map the action based on the observation which is equal to the states of the system. However, in POMDP, the agent has no access to the true system state and the agent only receives the observation which is generated from the latent state of the system [3]. In this case, the agent is required to construct its state representation from the available information to restore the MDP condition. This state representation can be described in the same state space as the systems but also it can be in the encoded internal state space.

One of the approaches to address POMDP is using sequential information which the agent has experienced on its

* *Citation:* This work has been submitted to the IEEE for possible publication. Copyright may be transferred without notice, after which this version may no longer be accessible."

trajectory. By processing the sequential information, the agent could generate the internal state representation and restore the MDP condition. The recurrent neural networks or other advanced gated recurrent neural networks such as Long-Short Time Memory (LSTM) and Gated Recurrent Unit (GRU) can process the sequential data by carrying hidden states. These networks are implemented RL and they have shown improved performances in various POMDP environments [4, 5, 6, 7]. However, most of the development only utilizes sequential observation and not uses all available information. There are also other recent approaches to work on time series data in this context e.g., transformer [8, 9] and Liquid Time-constant Network [10].

Although many algorithms have been developed to deal with POMDP, further investigation and development are required regarding the robustness under disturbances. Very little research has studied effects of selection of information, length of the utilized action/observation sequence, and network structure on the robustness. Also, the analysis of the disturbance characters is lacking although algorithms are tested in POMDP environments. Robustness is an important element in practical applications. Although the policy is optimized in certain conditions, the solution does not necessarily remain optimal once the configuration of the environment varies. The recent discussion of Sim2Real transfer is more focused on increasing the fidelity of the simulator [11, 12] but it is not possible to model the real world perfectly [13]. Therefore it is important to increase the robustness of the trained system.

The robust system with generalizability can keep the performance well in any condition once it is trained. In an effort to build such generalizability into the system, we consider the robustness of optimality under the specified non-static environment in this work. Namely, the networks are evaluated based on the achieved total reward per episode in POMDP environment. The robust agent, in this study, should dynamically adjust the policy in the environment with disturbances.

Firstly, the related background knowledge is briefly explained in Section 2. Secondly, we discuss the importance of including action sequences in the POMDP framework in Section 3. Then, we evaluate one of the existing algorithms which has the LSTM layer and discuss the effect of the sequential information component and the length of time window to look back on different types of disturbances in Section 4. Section 5 proposes a new structure of the network to improve the existing algorithm. With this structure, the sequential information is processed individually in the actor and critic network. Also, in Section 5, we discuss a different methodology to share the internal state representation between both networks. Finally, all developed algorithms are compared and evaluated in Section 6. The contribution of this work can be summarised as follows:

1. We explain how the selection of information matters in solving POMDP. Past action sequences can help to increase the robustness of optimality due to their causality in the environment (Section 3). The effect of information on the robustness is identified and discussed (Section 4).
2. The network structure to attend to the sequential data is discussed carefully in Section 5. By following the evolution of internal state construction, we show that it is more reasonable to treat the past and current information as one sequence instead of processing them independently.
3. When LSTM cells are applied in the network, the sequential information is carried by hidden states h_t and cell states c_t . We propose a new algorithm to train the critic network based on the generated hidden states from the actor network (Section 5). The evaluation of the proposed methodology shows the possibility to utilize them as the initial state of LSTM cells in training. This approach makes it possible to avoid reprocessing the sequence at each network during the training.

2 Preliminary

The neural network and algorithm related to this work is introduced in this section. Further basics of RL can be found in [14].

2.1 Recurrent Neural Network

RNN is nowadays a widely used technique, yet it is worth briefly revisiting the concept since later discussion and algorithm development require the detail of RNN. RNN is a suitable learning network to deal with sequential data as input. Fig. 1 contrasts the difference between Feedforward Neural Networks (FNN) and RNN. Unlike FNN, RNN carries the context of sequential observation and make predictions. On the other hand, FNN treats every input independently from other sequentially provided inputs and it returns outputs only depending on the current neural state [15]. For example, the text generation application requires the prediction of the next word coming based on not only the last word but also the previous words. RNN can predict output as a function of the current input and the inherited hidden states that capture contextual information from all of the previous inputs based on its trajectory. As a deep neural network application, RNN is widely applied for cases where sequential data is involved in the prediction (e.g. audio speech, time series prediction). In Fig. 1, the hidden state h_{t-1} from the hidden layer is carried

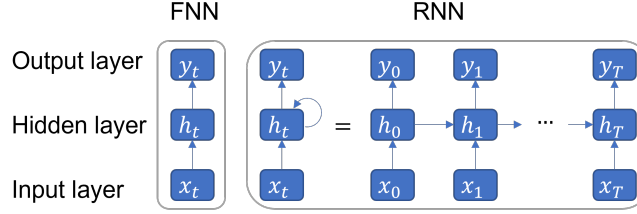


Figure 1: FNN and RNN diagram

to generate output data y_t at the output layer when new input data x_t enters in RNN. In case of RL, input data x_t can be direct observation o_t or output from the previous layer originated from o_t . The original RNN suffered from a vanishing gradient problem where the gradient becomes extremely small and has no effect on backpropagation through time (BPTT). To address this issue, advanced recurrent networks, such as Long Short-Term Memory (LSTM) network [16] and Gated Recurrent Unit (GRU) network [17], with the gating network were developed. Fig. 2 shows the simplified schematic of LSTM cell. LSTM consists of three gates named input gate, output gate and forget gate and inherits hidden states h_t and cell states c_t to make an estimation for the next time step. More specifically, the input gate decides what information should be stored in the cell state c_t based on the current input and inherited hidden states. If the value is closer to 1, the particular information generated from input data x_t and previous hidden states h_{t-1} has more weight to update the cell state. Also, forget gate selects how much information from the previous cell states should be forgotten or kept. If the values are closer to 0, less information from the previous cell states c_{t-1} is kept in the updated cell states c_t . By using these two gates, the network can selectively process the most informative (related) data in the input sequence. The output gate finally weights the information to be taken from the cell state as an output. GRU also has a similar gating mechanism. Due to these gates, LSTM and GRU can effectively carry the information and have less chance to face the gradient vanishing problem. In this work, LSTM is utilized in one of the layers of the neural networks to approach POMDP. The network is trained via BPTT, which goes back through the entire sequence used to generate the output.

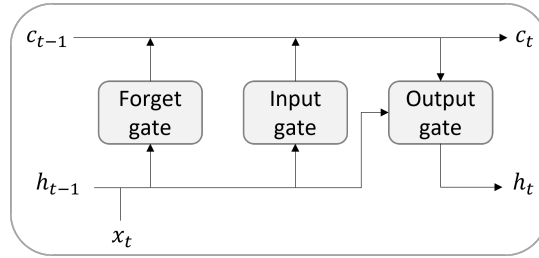


Figure 2: Simplified LSTM cell schematic

2.2 Twin Delayed Deep Deterministic policy gradient algorithm

The developments in this work are based on Twin Delayed Deep Deterministic policy gradient algorithm (TD3) [18]. The schematics of TD3 are illustrated in Fig. 3. o_t , a_t , r_t and a'_t in the figure represent observation, action, reward and action generated by target actor network at time step t . DDPG [19] showed great performance with an efficient number of iterations. However, the issue of Q-learning overestimation remained. In [18], this issue was investigated and the extended algorithm was presented as TD3. Like in the Double Q-learning algorithm [20], TD3 has a double critic network. Each critic network has a target critic network and actor network also consists of the target network and behavior network. Thanks to several modifications, TD3 showed better performance in achievable total reward compared to the other latest deep RL algorithms. Although the original TD3 might suffer from performance degradation, there are only few developments for TD3 to solve POMDP.

2.3 LSTM-TD3

In [21], the LSTM layer was implemented in the TD3 algorithm which is named LSTM-TD3. LSTM-TD3 has LSTM layers in actor and critic networks. The past sequential information is processed through LSTM layer. Processing sequence in an entire episode is time-consuming to train the network. Hence, in LSTM-TD3, the networks process

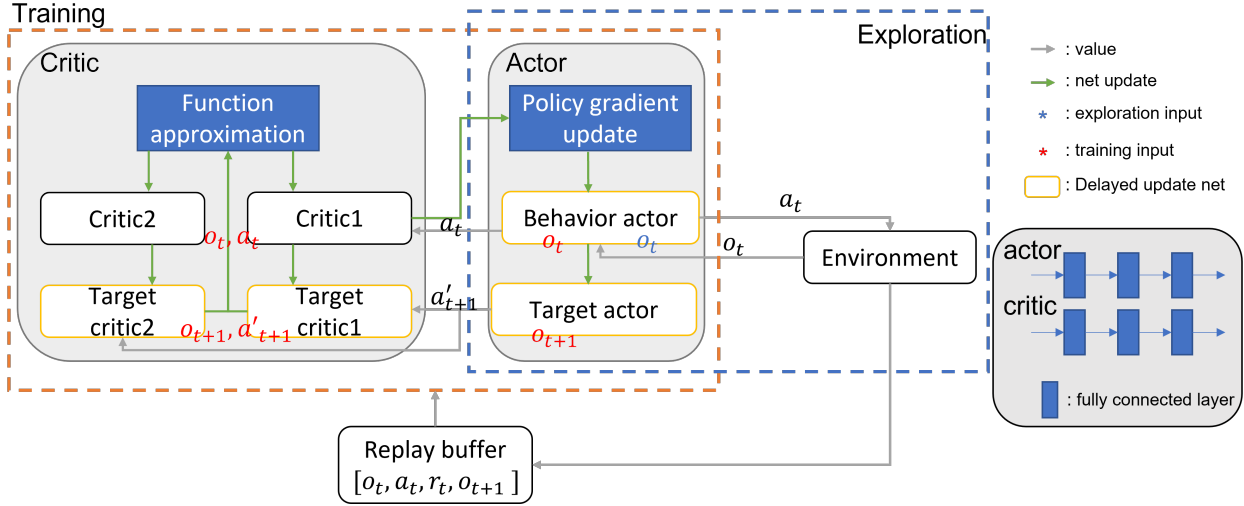


Figure 3: TD3 schematics

partial trajectory instead of entire trajectory up to the current time step by setting a specific sequence length l to generate the action from the policy and to roll out the trajectory during the update as a hyper-parameter. This method to train a network with the partial history of a specific length is also applied in [6] as described in Section 7. Another aspect to be mentioned is that LSTM-TD3 has a double input channel as network architecture as shown in Fig. 4. The input data for the first input channel is sequential past information $[o_{t-l:t-1}, a_{t-l:t-1}]$ from the memory

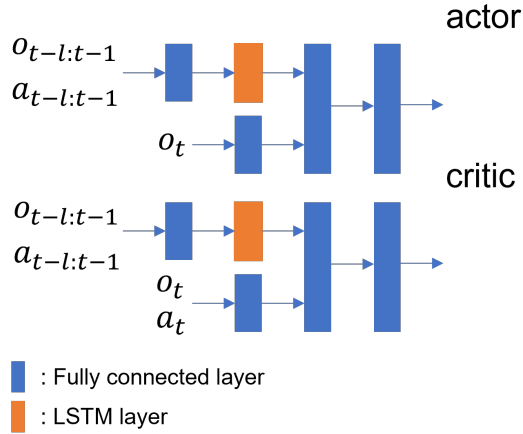


Figure 4: LSTM-TD3 schematics

and the second input channel takes the current information $[o_t, a_t]$. The expression $o_{t-l:t-1}$ and $a_{t-l:t-1}$ describes the sequential observation and action between time step $t-l$ and $t-1$ respectively. This structure was selected in order to prioritize the most recent observation since it is considered that the recent observation is more valuable in decision-making than earlier observations. Note that this hypothesis is questionable because it might not be true that the latest observation is more informative to reveal the true state of the system. This will be discussed in detail in Section 5. LSTM-TD3 [21] was tested for robot locomotion tasks in open AI gym simulation environment [1] with several types of POMDP such as removing one of the state elements from the observation and adding random noise to observation. Especially in the scenario where one or all of the observation is lost with probability p , LSTM-TD3 showed greater performance compared to original TD3 and other Deep RL algorithms.

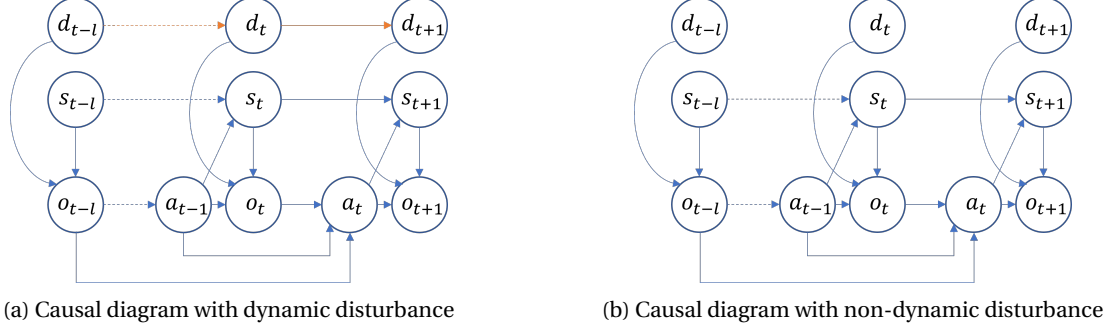


Figure 5: Causal diagram

3 Dynamic RL

The challenge of POMDP in this study is that we have no access to the true state of the system s_t due to the disturbances in observations. In our scenarios, disturbances are realized by stochastic noise or dynamic noise, or by hiding one of the elements of the observation. The details of disturbances are defined in Section 4. If s_t can be estimated or represented in an internally encoded format, it is possible to restore the MDP condition. Then, an already established RL algorithm can be utilized to identify the (sub-)optimal policy. Therefore, recovering the MDP condition through certain architecture design choices such as the definition of input/output variables should be important for the policy robustness. Hence our focus is to develop a RL agent which can dynamically adapt to the observation containing the disturbance with their own dynamics. To make a dynamic RL agent, the system should be able to generate the internal state representation by assessing causal information from the trajectory.

3.1 Causality and Statistics

The dichotomy of statistics and causality are emphasized in [22]. A statistical model works on the joint probability of observed variables. A causal model, on the other hand, assumes that certain variables are unobserved. The causal analysis enables inference of dynamics of events under changing conditions, not only the likelihood of events under static conditions.

In MDP, the static transition model is available (e.g., $P(o_{t+1}(=s_{t+1})|o_t(=s_t), a_t)$). However, in POMDP with non-static disturbances, the model of the world dynamically changes. Therefore, it requires an additional mechanism to identify the causal effect and recognize the pattern based on available information in the past and current.

3.2 Analysis of disturbance

When the decision-making is performed based on information on the trajectory, the causal system is illustrated in Fig.5. In this work, the considered disturbances can be categorized into two. The first case is where the disturbance can be described by a dynamic model (Fig. 5a). Therefore, the trained agent may be able to learn a model comprising the system and the disturbance. The second case is where the disturbance does not have a temporal correlation between them and cannot be modeled (Fig. 5b). In this case, the agent should learn to eliminate the effect of the disturbance to reveal the true state. The trained agent in the environment of which category described in Fig. 5a might show generalizability in the environment where the existing disturbance has temporal correlation but not the other one. This will be demonstrated in Section 6.

3.3 POMDP formulation

In general, the POMDP model is defined as 6-tuple $\langle \mathcal{S}, \mathcal{A}, \mathcal{O}, \mathcal{T}, \mathcal{Z}, \mathcal{R} \rangle$ [2], where

- \mathcal{S} is the state space,
- \mathcal{A} is the action space,
- \mathcal{O} is the observation space,
- $\mathcal{T}(s_t, a_t, s_{t+1})$ is the state transition which is a conditional probability distribution $P(s_{t+1}|s_t, a_t)$,
- $\mathcal{Z}(s_{t+1}, a_t, o_{t+1})$ is the observation function which is a conditional probability distribution $P(o_{t+1}|s_{t+1}, a_t)$,
- \mathcal{R} is an immediate reward function which represents $\mathcal{R} = \mathbb{E}[r_{t+1}|s_t, a_t]$.

When observations are corrupted by additive dynamic disturbances, the observation function \mathcal{Z} is not static. Namely, the observation function can be described as $P(o_{t+1}|s_{t+1}, a_t, d_t)$. In addition, if the disturbance is modeled and it is independent of the states and action, a new disturbance transition function, which represents a conditional probability distribution could be introduced.

3.4 Information states, belief states in POMDP

In the context of dynamic programming, the optimal controller in POMDP can be separated into two parts; (a) an estimator and (b) an actuator [23, 2]. The information available at time t is called complete information state I_t^C [24] which consists of all historical observation and action i.e., $I_t^C = (o_{0:t}, a_{0:t-1})$, where $o_{0:t} = o_0, \dots, o_t$ and $a_{0:t-1} = a_0, \dots, a_{t-1}$. In the case of POMDP, the estimator could make the conditional expectation $\hat{s}_t = \mathbb{E}(s_t|I_t^C)$. The challenge of utilizing the complete information states is that the size of the data expands as time elapses. To resolve this issue, quantities known as sufficient statistics are normally considered. The sufficient statistics has a smaller dimension and preserves the essential content of I_t^C . The sufficient static is generated at the estimator and the actuator generates control inputs to the system based on the sufficient static. In the standard POMDP model, a belief state b_t is commonly used as sufficient statistics. The belief state assigns conditional probabilities of every possible state [25]. As illustrated in [2], the policy of the agent receives the belief states to make optimal decisions. The belief states could be recursively updated via Bayesian inference. The update of belief states can be described as (1).

$$\begin{aligned} b_{t+1}(s_{t+1}) = P(s_{t+1}|o_t, a_t, b_t) &= \frac{P(o_t|s_{t+1}, a_t, b_t)P(s_{t+1}|a_t, b_t)}{P(o_t|a_t, b_t)} \\ &= \frac{\mathcal{Z}(s_{t+1}, a_t, o_t) \sum_{s_t \in \mathcal{S}} \mathcal{T}(s_t, a_t, s_{t+1}) b_t(s_t)}{\sum_{s_{t+1} \in \mathcal{S}} \mathcal{Z}(s_{t+1}, a_t, o_t) \sum_{s_t \in \mathcal{S}} \mathcal{T}(s_t, a_t, s_{t+1}) b_t(s_t)} \end{aligned} \quad (1)$$

3.5 Identification of transition model

The objective of RL is to maximize the future cumulative reward G_t by learning policy π . In model-based RL, it is solved by decomposing the problem into learning and planning. From learning, the transition model is explicitly obtained from experience, and the value function is established based on the learned model in planning. The agent is directly trained from the experience in model-free RL. The transition model and its update operation formulated in (1) is not required. However, the concept itself is still applicable since it is established based on it as described in Section 2. In model-free RL, the model is internally generated based on the collected data directly. Action is the element of the transition model and, therefore, it is part of a recursive update. Thus, it is clear that taking action sequences in model-free RL will help to improve the robustness of optimality in POMDP.

In either case of using complete information state I_t^C or belief state b_t , identification of the dynamic transition model relies not on only the historical information of observation, but also that of action, since both have causal connections on the current observation as depicted in Fig. 5a. As we are considering the environment where the observation is disturbed, our discussion is focused on generating internal representations of s_t which is symbolized by s_t^* in the rest of this paper. The key idea is to formulate a structure of an RL agent which can dynamically adapt the state representation s_t^* on given disturbances.

3.6 LSTM to reflect the sequence on the internal representation

When the model of the system is not available, s_t^* could be generated via RNN or enhanced RNN by processing the sequential input. s_t^* could contain the identified information regarding the pattern of the dynamic model of the system and the disturbance or distilled information which is less affected by the disturbance. Most of the existing RL algorithms with RNNs only utilized the sequential information of observation and there are only very few cases taking action sequence as input. We suggest utilizing the sequence of action based on the above discussion in this study. Therefore, the effect of sequential action inclusion with the LSTM-TD3 algorithm [21] is investigated in the next section.

4 Action inclusion

In the previous section, we have discussed that the belief state evolves based on the observation and action on the trajectory. In this section, the impact of the inclusion of the action sequence is demonstrated using LSTM-TD3. Also, the effect of the length of the sequence for the individual disturbance condition is investigated.

4.1 Length of sequence

When the partial trajectory is taken as the input sequence, the selection of its length l can be a design parameter as in LSTM-TD3. In general, RL algorithms with a RNN layer require repeating either entire or partial episodes during the update in order to train the network via Back Propagation Through Time (BPTT). When entire episodes are repeated in training, it can be considered that the agent is trained using complete information I^C . As stated in Section 3, the size of I^C increases as time elapses. Thus, repeating entire trajectories to update the network is a time-consuming process. In case of the on-policy algorithm with RNN, utilizing I^C might be a more natural approach since it follows the same trajectory during the training. Several works have explored the methods combining RNN with on-policy algorithms (e.g. with PPO[26] and A3C [27]). However on-policy algorithms are much less sample-efficient compared to off-policy algorithms.

For state value function based algorithms, parameter sharing is a common technique where the actor and critic share the same network parameters and only the last layer of each network is different. However, this technique is not as common for action value function based algorithms like TD3 since the parameter sets are different between actor and critic networks. When parameter sharing is not used, the same trajectory needs to be repeated multiple times to update multiple networks.

If the whole episode is repeated, the benefit provided by random sampling can be lost in the experience replay which is the mechanism for improving data efficiency and stability. Experience replay effectively minimizes the correlations between samples [19] so that the data distribution becomes closer to independent and identically distributed (i.i.d.) condition which is preferable in RL. In [28], it is concerned that if the whole trajectory is sampled together, the bias in the learned policy might become severer in the update because the state distribution under the current policy no longer corresponds to the one from the replay buffer.

If a few steps of sequential data are randomly sampled as a unit, the sample correlation issue could be mitigated. This approach captures a shorter history of fixed length in the environment. LSTM-TD3 offers the opportunity to define the length of the sequence. The agent should be provided with enough length of sequential data so that it can capture the characteristics of the system and the disturbance. In the experiment in this section, the relationship between several characteristics of the disturbance and the length of sequence that is provided to the network is investigated.

4.2 Experiment

To validate the discussion in Section 3 and investigate the effect of including action sequence on the different types of disturbances, we compare learning trajectories of the LSTM-TD3 algorithm are compared between with or without the past action sequence in the first input channel (see Fig. 4) in classic control "Pendulum" environment from OpenAI gym. In this environment, the observation consists of three elements $[x, y, \dot{\theta}]$, where x and y represent the position of the free end of the pendulum and $\dot{\theta}$ is its angular velocity. The action is defined as the torque to be added and the agent learns to keep the pendulum upright from a random initial condition. The definition of the "Pendulum-v0" environment is summarized in Table 1.

The motivation for this work is to develop an algorithm which robustly provides optimality under the presence of

Table 1: "Pendulum-v0" environment definition

action	torque	min -2.0	max 2.0
observation	$x = \cos\theta$	min -1.0	max 1.0
	$y = \sin\theta$	min -1.0	max 1.0
	angular velocity	min -8.0	max 8.0
reward	$r = -(\dot{\theta}^2 + 0.1\theta^2 + 0.001(\text{torque})^2)$		
termination	at 200 time steps		

disturbance. As summarised in Table 2, we classified disturbance under condition into five types: "temporal bias", "temporal sinusoidal wave", "random sinusoidal wave", "noise" and "hidden" conditions. In the "temporal bias" and the "temporal sinusoidal wave" cases, the observation of x and y are disturbed for specific lengths and times at random time steps by additive constant biases and sinusoidal waves. In the "random sinusoidal wave" case, the sinusoidal wave is randomly configured at each episode and all three elements are disturbed. In the "noise" case, zero-mean Gaussian noise with standard deviation σ , is added to each element of the observation during the entire episode. In the "hidden" condition, $\dot{\theta}$ is removed from the observation during the whole episode and the dimension of the observation becomes two. Scenarios 1,2, and 3 in Table 2 are the cases where the disturbance has its dynamics and patterns could be identified from the observation. The other remaining two cases have no dynamics in the

disturbance. The networks should rather work on recovering the dynamics of the system by eliminating the effect of the disturbance from the observation than establishing a model comprising the system and disturbance.

Table 2: Test scenario

Scenario	Name	Description
1	temporal bias	Disturbance defined by $A \in [0.5, 1.0]$ appearing randomly is added to observation in x and y lasting 3 time steps for 10 times per episode.
2	temporal sinusoidal wave	Disturbance defined by $A \sin 2\pi t / T$ ($A = 1$ and $T = 70$) which starts appearing at randomly chosen time steps for the period of T , is added to observation x and y .
3	random sinusoidal wave	Disturbance randomly defined in every episode by $A \sin 2\pi t / T$ ($0.5 \leq A \leq 2$ and $10 \leq T \leq 100$) which starts appearing at random time step for the period of T , is added to all 3 observation elements.
4	noise	Noise defined by zero-mean normal distribution with standard deviation $\sigma \in [0.5, 1.0]$ is constantly added to all 3 observation elements.
5	hidden	Angular velocity $\dot{\theta}$ is removed from observation.

4.3 Results and analysis

Fig. 6 to Fig. 11 show normalized learning trajectories after 5 trials of the LSTM-TD3 algorithm in the discussed scenarios. The orange lines, labeled "w/o action", show the case where the sequential action information is excluded. Namely, the first input channel of actor and critic networks process only sequential $l - 1$ length of historical observation $o_{t-l:t-1} (= o_{t-l}, \dots, o_{t-1})$. The blue lines, labeled "w/ action", show the case which has historical action $a_{t-l:t-1}$ as additional information. The columns represent the length of the history to be processed. Fig. 6 and Fig. 7 illustrate the results of the MDP case and the "temporal bias" case respectively. In the MDP case, LSTM-TD3 with or without action performs the same. Also, the final performance at the end of training in the "temporal bias" case did not show obvious differences. In this condition, a constant value is added for three time steps that randomly start appearing 10 times. Since the observation is biased by a constant value, the observation is still almost unique. Therefore, it can be considered to be similar to the MDP condition.

Fig. 8 shows the results of the "temporal sinusoidal wave" scenario. As l gets longer, the robustness improves. The wavelength of the defined sinusoidal wave is 70. Longer l helps to identify the system dynamics and the disturbance dynamics. Also, the case with action sequence included as the input to the agent achieved higher total rewards. The result indicates how the choice of information affects the robustness.

Fig. 9 represents the learning trajectory of the "random sinusoidal wave" scenario. Establishing the observation function in this scenario is much harder as compared to the "temporal sinusoidal wave" due to the infinite variety of sinusoidal waves. It requires the agent to dynamically adapt to the environment based on causality of action and observation and hence, the network with action sequence reaches better optimality.

Fig. 10 illustrates the learning trajectory under the "noise" condition. This scenario is more challenging than the "temporal sinusoidal wave" since there are no specific dynamics in the disturbance and all of the elements of the observations are constantly disturbed. Although the network considering sequential action information performs better, the performance degrades with the larger variance of the noise. The performance improves with longer l . Longer sequential data contributes to extracting the system state transition characteristic and eliminating the effect of the noise in LSTM. In the white noise case, some data randomly contain less noise. By focusing on these data and putting less focus on more noisy data, the underlying pattern can be restored. When the length of the input sequence is longer, it has more chance to have informative data which is less affected by noise. In addition, as more episodes are experienced, degradation of achieved total reward was observed in the "noise" scenario. This would be due to the occurrence of overfitting. It could be prevented by changing the network configuration, e.g., reducing the number of parameters, and adding dropout layers.

Fig. 11 presents the result of the "hidden" scenario. The final performance is the same regardless of the action inclusion and length of the sequence. In this environment, only current observation o_t and one step before o_{t-1} should be sufficient to restore $\dot{\theta}$ since θ is updated as $\theta(k+1) \leftarrow \theta(k) + \dot{\theta}(k+1)dt$. The formula only requires the previous observation to restore $\dot{\theta}$ from the equation and therefore the performance is not affected by l . However, the past action information is making the learning process more efficient. The network does not have this mentioned interpretation and the reward signal is mixed with θ , $\dot{\theta}$, and torque. The inclusion of action information could make learning efficient because the network learns to process the dynamics under more specific conditions. The most

reasonable network structure to include this interpretation might rather just consist of fully connected layers by having the input of $[x_t, y_t, x_{t-1}, y_{t-1}]$ because the sequential process is not required.

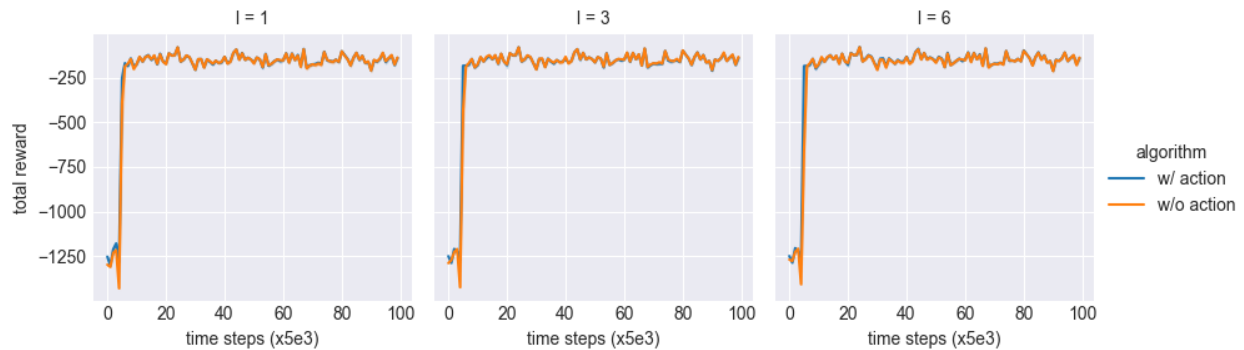


Figure 6: MDP

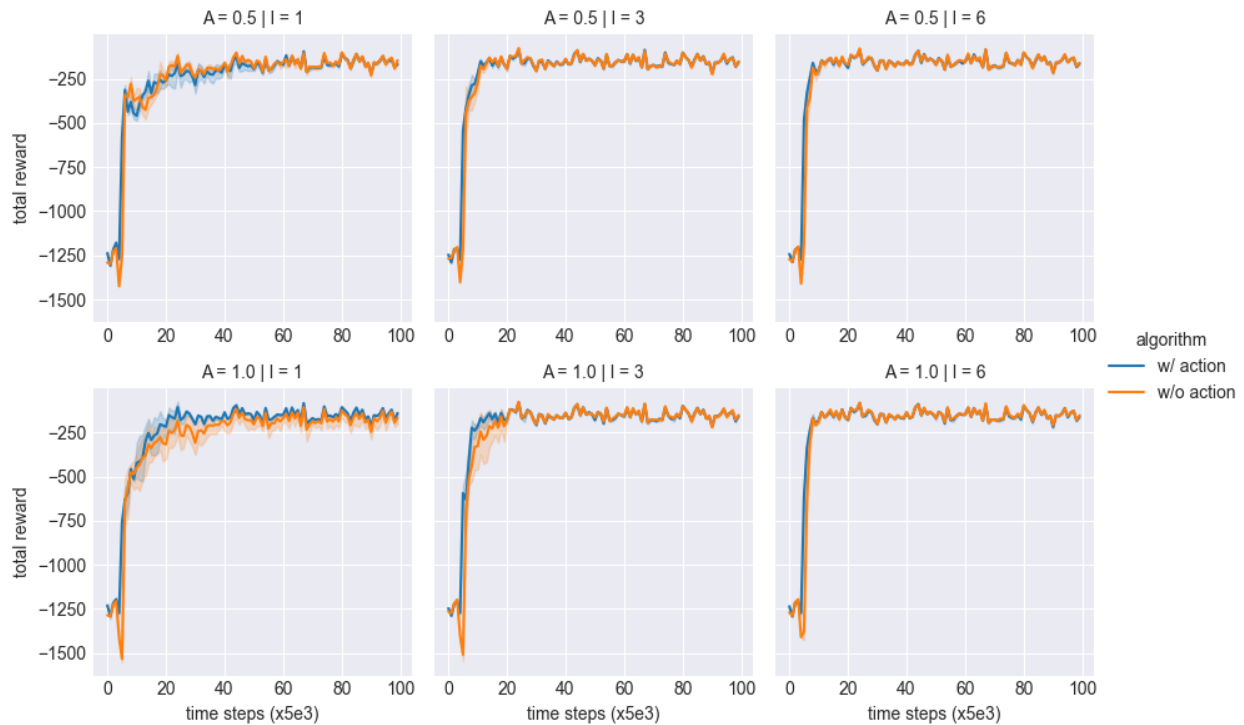


Figure 7: temporal bias

5 Structure

In Section 4, we demonstrated that including the action sequence can improve the robustness of learning. In this section, let us discuss the structure.

5.1 Interpretation of LSTM-TD3

The LSTM-TD3 has two input channels in both actor and critic networks. They could be interpreted that the first input channel to generate s_{t-1}^* from complete information $I_{t-l:t}^C$ taken from the memory. Then, the s_{t-1}^* is updated

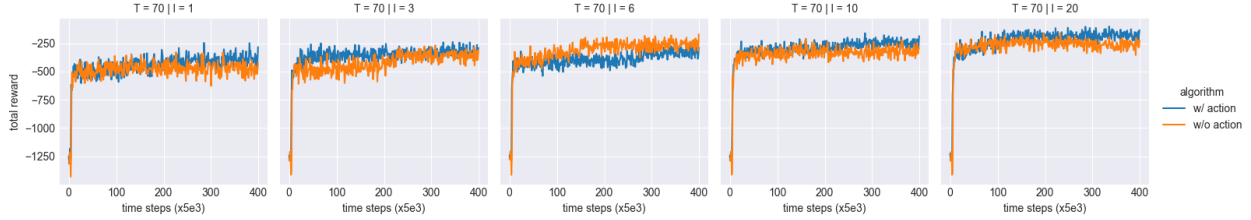


Figure 8: temporal sinusoidal wave

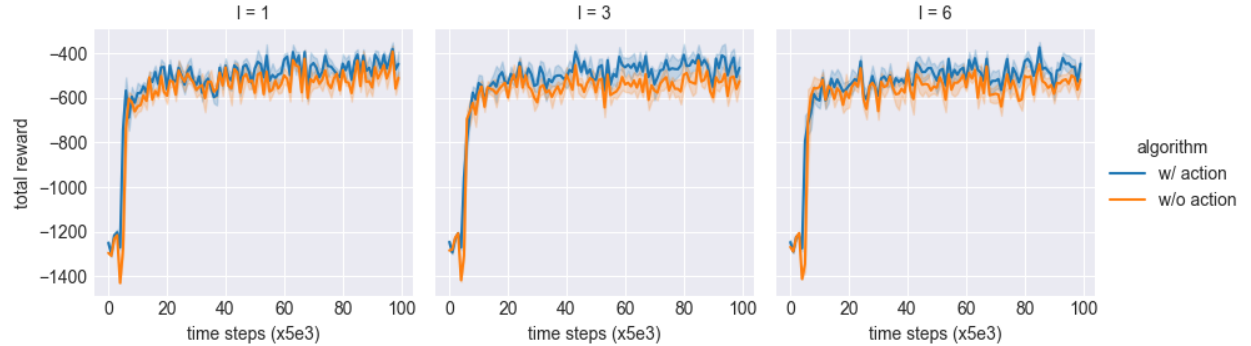


Figure 9: random sinusoidal wave

to s_t^* by combining the current observation information from the second channel at the actor. Our hypothesis is that it might not be necessary to have a double-headed structure as presented in Fig. 4 because the information up to the current time step can be treated as one sequence according to the generation of the information states.

5.2 Modified LSTM-TD3

Based on this hypothesis, this paper proposes an actor network with a single input channel as illustrated in Fig. 12. This input channel processes $I_{t-l:t}^C = (o_{t-l}, \dots, o_t, a_{t-l-1}, \dots, a_{t-1})$. Internal state representation s_t^* is generated in the process of the LSTM layer and action is decided based on s_t^* by the succeeding layers. For the critic network, two types of structure are considered. LSTM-TD3_{1ha2hc} (1 headed actor and 2 headed critic) in Fig. 12a has a clearer interpretation for s_t^* to the information states. s_t^* is generated in the same way as actor network at the first input channel and it is concatenated with the processed a_t at another input channel. The last two layers can be understood as $Q(s_t^*, a_t)$. On the other hand, LSTM-TD3_{1ha1hc} has single input channel and modified complete information $I_{t-l:t}^C = (o_{t-l}, \dots, o_t, a_{t-l}, \dots, a_t)$ is taken as input. $I_{t-l:t}^C$ differs from the generation of s_t^* based on the Bayesian inference and hence, the output from the LSTM layer is described as sa_t in the figure. However, the definition of action value function Q is the expected return at s_t , taking action a_t when following policy π . When the critic network is given with the trajectory, $I_{t-l:t}^C$, which is the combination of o_t and a_t from π , it should be able to still generate the expected return for π .

Unlike the original LSTM-TD3, LSTM-TD3_{1ha2hc} and LSTM-TD3_{1ha1hc} do not have an explicit intention to prioritize the current information. These proposed algorithms follow the update of the belief state and let LSTM to evaluate the importance of the data. Moreover, since the system model does not change in any time step, all data in a sequence should be treated in the same path. Training the agent with separate sequences might be more complicated because the data is processed differently and combined which might be unnecessary according to the belief state update. Therefore, LSTM-TD3_{1ha2hc} and LSTM-TD3_{1ha1hc} are expected to show better robustness.

5.3 H-TD3 algorithm

The previously discussed algorithms generate s_t^* in actor and critic networks independently by taking complete information at each network. Particularly, we have introduced the interpretation where s_t^* is produced in the LSTM layer at actor network. The research question to be also investigated is whether or not it is necessary to have a different representation of s_t^* between the two networks. If s_t^* generated from the actor network can be shared with

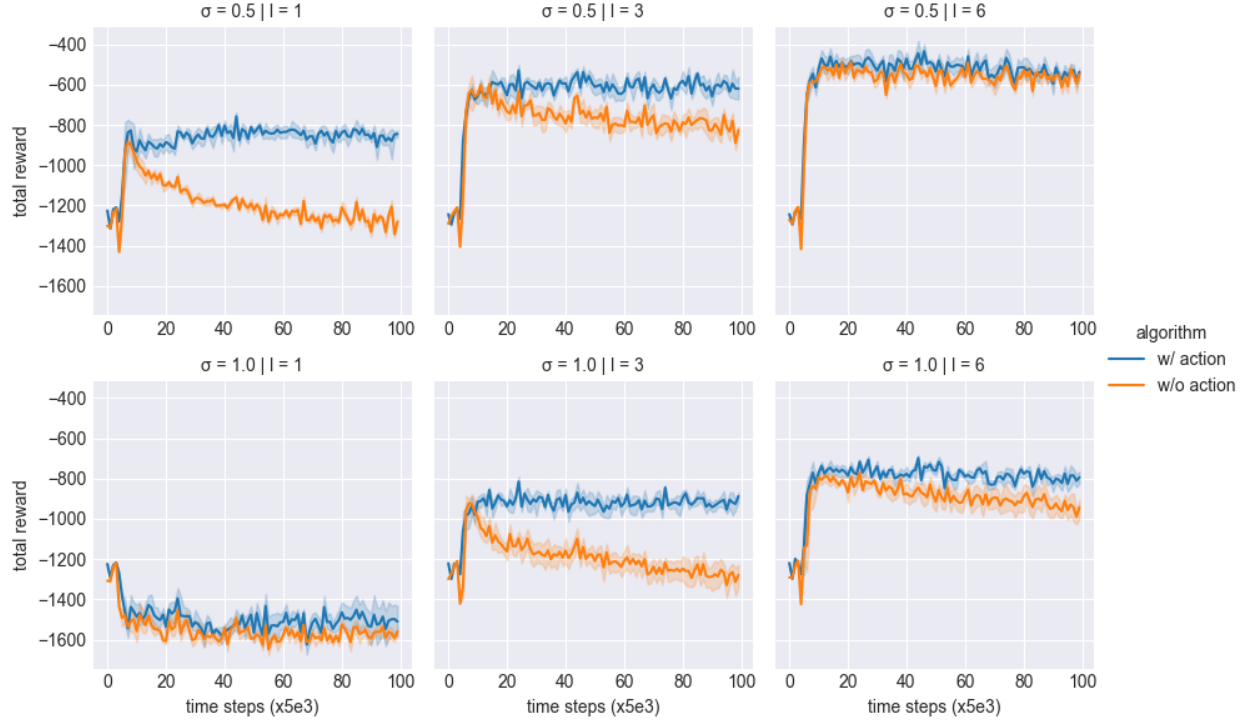


Figure 10: noise

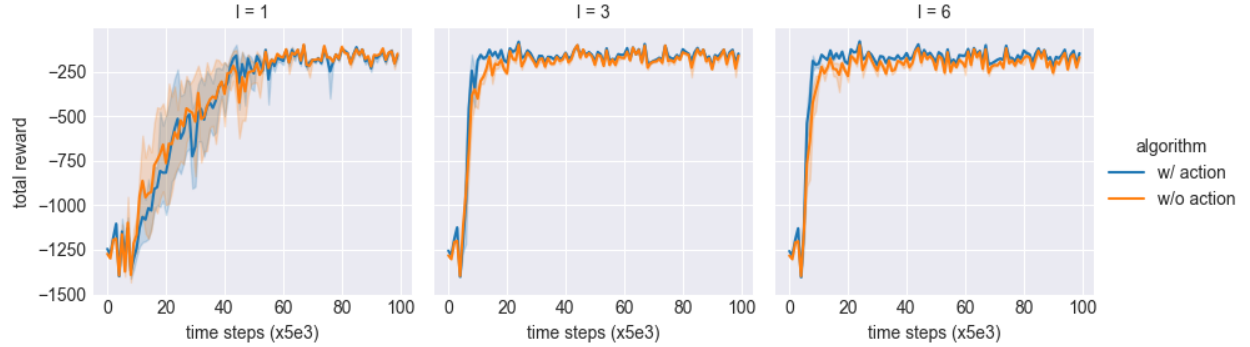


Figure 11: hidden

the critic network, it will drastically reduce the computational costs. Because TD3 has double critics as seen in Fig. 3, $I_{t-l:t}^C$ is processed four times at each critic network during the update. Hence we propose, a new algorithm, named H-TD3 (hidden-state-based TD3) in which the critic networks are trained based on the shared s^* from the behavior actor network during the exploration.

Here, we consider the same network structure with LSTM-TD3_{1ha1hc} which has a LSTM layer with a single input channel for the critic network as it is illustrated on the right side of Fig. 13. The main diagram of Fig. 13 describes the data flow of the H-TD3 algorithm. During exploration, the behavior actor and environment interact and the collected data is stored in the replay buffer. In addition to the normal data set, the hidden state and the cell state of the LSTM cell are stored. These states are generated at the behavior actor network when LSTM processed the sequence of $a_{t-l-1:t-2}$ and $o_{t-l:t-1}$. During the training, the critic network is trained based on this tuple. Critic networks take a_t and o_t as input data as the original TD3 algorithm. However, the LSTM cell is initialized with the stored $(h_{t-l:t-1}, c_{t-l:t-1})$. In this way, input data a_t and o_t is treated as if a continuous sequence of $a_{t-l-1:t-2}$ and $o_{t-l:t-1}$ without repeating the entire trajectory between $t-l$ to t . In the same way, at the target critics, the target Q-values are calculated based on input data a_{t+1} and o_{t+1} with initialized LSTM state with $(h_{t-l+1:t}, c_{t-l+1:t})$. The

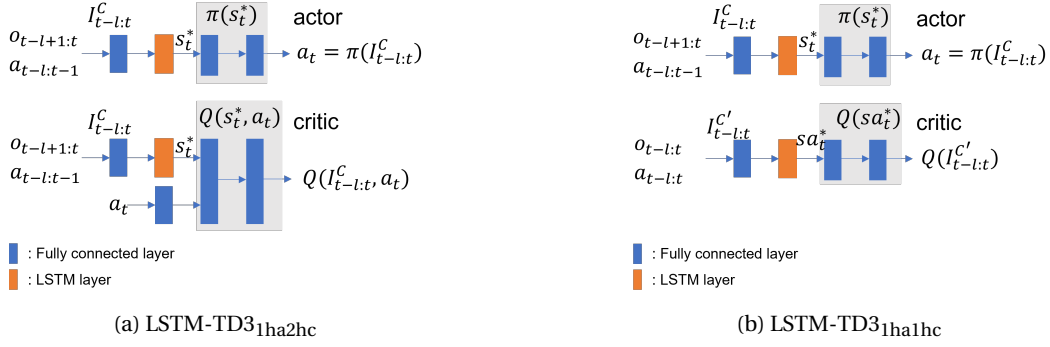


Figure 12: Modified LSTM-TD3 structure

critic network is required to learn parameters based on $(a_t, o_t, h_{t-l:t-1}, c_{t-l:t-1})$. The criticism of this approach may be the dismissed action a_{t-1} and a_t at critic and target critic networks respectively. However, if the hidden states $(h_{t-l:t}, c_{t-l:t})$ of LSTM after processing all sequence $a_{t-l-1:t-1}$ and $o_{t-l:t}$ are used to initialize critic networks, o_t is counted twice and it would break the sequence at the critic. Another possibility could be to limit the input just to a_t , but changing the character of input data to LSTM for the given $(h_{t-l:t}, c_{t-l:t})$ in critics would add difficulty in learning. During the development, we observed the degradation of performance in both cases compared to using $(h_{t-l:t-1}, c_{t-l:t-1})$.

Considering the developed LSTM-TD3_{1ha2hc} and LSTM-TD3_{1ha1hc}, the output data from LSTM in actor network is the last hidden states h_t after processing l length of the sequential input. After the LSTM layer, h_t is carried to the following last two layers. Hence, the simplest method for the critic networks to learn based on the shared s^* would be taking h_t as input data at the critic network in addition to the current observation. However, this operation would extend the input dimension excessively as the dimension of the hidden state is usually much larger than that of the input. It increases the difficulty to train the network and the risk of failure of learning as known as the "curse of dimensionality". Training network with larger input dimensions increases the number of parameters drastically, leading to the much greater computational complexity of training. Also, ending up with over-fitting is a common issue. Therefore, it is more scalable to share the hidden and cell states produced in the actor network to initialize the hidden state of the critic network as in the proposed H-TD3 algorithm.

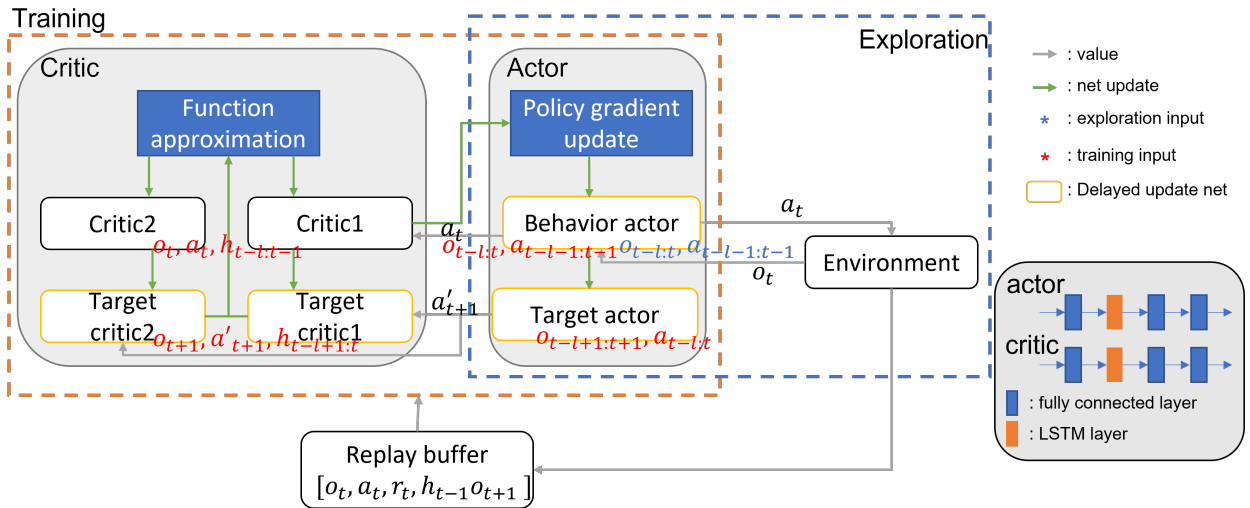


Figure 13: H-TD3 schematics

6 Experiment

6.1 Simulation set-up

In this section, the algorithms developed in Section 5 are tested in the "Pendulum" environment with disturbance conditions discussed in Section 4. The applied disturbance conditions are as follows:

- "temporal sinusoidal wave" with $\sin \frac{2\pi}{70} t$
- "random sinusoidal wave"
- A zero mean Gaussian "noise" with $\sigma = 0.5$
- "hidden"

6.2 Results

In Fig. 14, the learning trajectory of the proposed algorithms is depicted. The trajectories are averaged after 5 trials. The time window l is selected to be 1, 3, 6, 10, 20. In the array of figures, each row represents a disturbance condition and each column represents an algorithm. The algorithms compared are original LSTM-TD3 without past action sequence, LSTM-TD3 with past action sequence, LSTM-TD3_{1ha1hc}, LSTM-TD3_{1ha2hc}, H-TD3 and original TD3 from the left column. The disturbances are "temporal sinusoidal wave", "random sinusoidal wave", "noise" and "hidden" from the top. The number of the iteration varies depending on the disturbance conditions.

Fig. 15 shows the normalized total reward of the last ten records by taking algorithm types on the x-axis. Each figure describes the result of "temporal sinusoidal wave", "random sinusoidal wave", "noise" and "hidden" conditions respectively. The lines are drawn to compare the effect of the time window l .

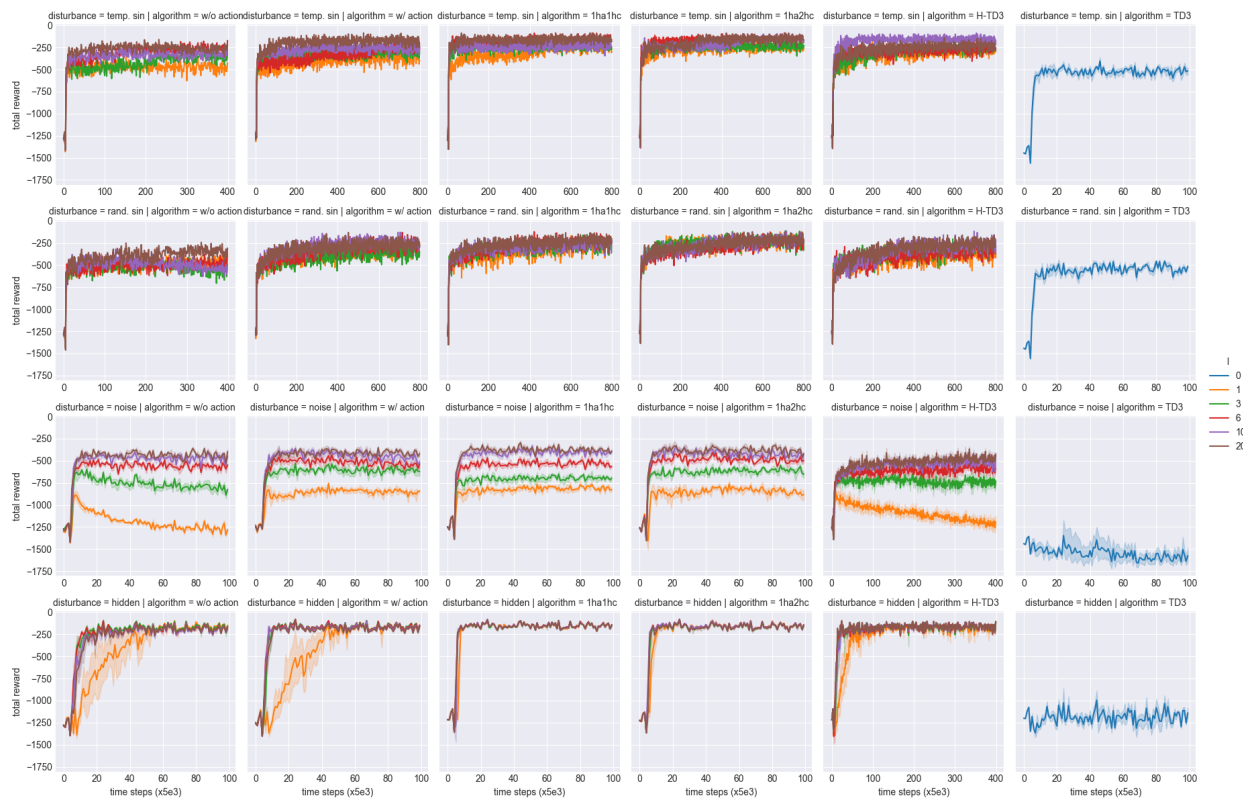


Figure 14: Learning trajectory

Overall analysis Compared with TD3, any algorithms with LSTM layer showed better performance in the tested POMDP conditions. Especially, in the "noise" and the "hidden" cases, TD3 failed to learn. The "noise" environment generates the reward given the noisy observation. Without having a sequence, it is difficult to learn since the

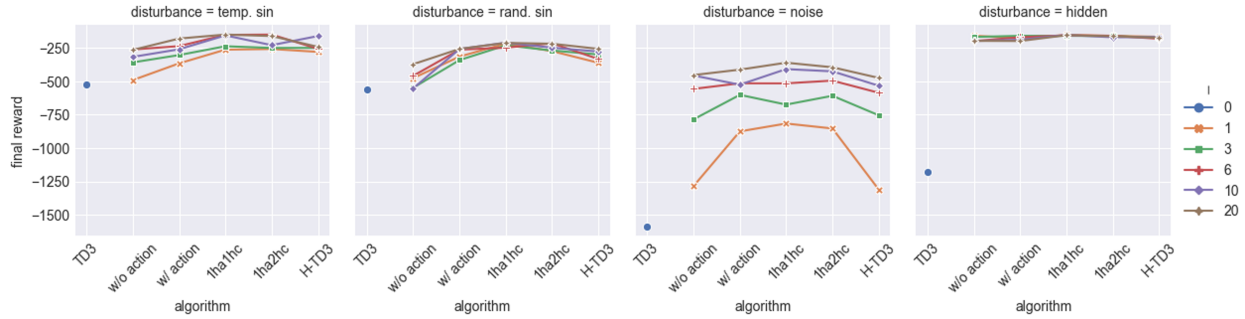


Figure 15: Final total reward

observation values are not unique to the reward signal. Also, the "hidden" without LSTM layer cannot recover information related to angular velocity which is part of the reward function.

As observed in Section 4, all algorithms with action sequences performed better than LSTM-TD3 without an action sequence. The midfield LSTM-TD3 (LSTM-TD3_{1ha1hc}, LSTM-TD3_{1ha2hc}) showed generally better performance compared with the original LSTM-TD3 with action sequence. From the results, it can be understood that it is better to treat the past sequence and current data as one sequence, unlike LSTM-TD3. LSTM-TD3_{1ha1hc} had the best robustness in the optimality of all algorithms. The simplicity of the structure could have helped the network to learn. H-TD3 algorithm presented a comparable result with LSTM-TD3 with action case except for the "noise" case. It proves that it is possible to learn from shared hidden states seen in H-TD3 results. However, H-TD3 showed a slower learning trajectory for a given number of iterations compared to the others in Fig. 14 due to the critic's dependency on the actor network to generate the hidden states and cell states. Interestingly, the results of the "noise" case in H-TD3 were significantly degraded and mostly worse than LSTM-TD3 without action sequence. In the H-TD3 algorithm, a_{t-1} is not included in the information. The effect of lack of this information could become prominent in some conditions as in the "noise" case.

Computational time and size Let us examine the computational time for training the network. Fig. 16 shows the comparison of the training time by taking LSTM-TD3 with $l = 1$ as the benchmark. Due to the added operations in the code, LSTM-TD3_{1ha1hc} and LSTM-TD3_{1ha2hc} have a larger iteration time. The code is not optimized and there is room for efficiency in computation. As shown in the figure, the H-TD3 offers a much shorter time per iteration and is less affected by the length l . It is because it does not require repeating the trajectory in critic networks.

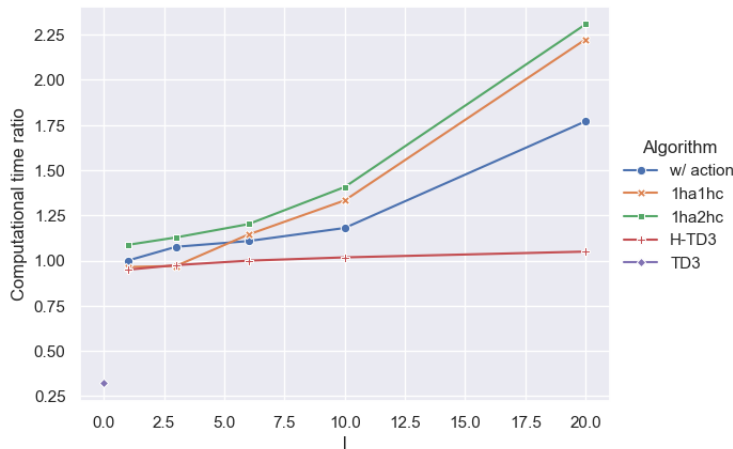


Figure 16: Iteration time comparison

Generalisability So far, the networks have been evaluated in the same environment where they were trained. However, in practice, the agent may experience different types of disturbances from the trained environment. For this reason, we tested how the networks trained in the "random sinusoidal wave" environment perform in "bias" and

"noise" cases and also newly introduced environments: "combinational sinusoidal wave" and "damped sinusoidal wave". In the "combinational sinusoidal wave", two randomly configured sinusoidal waves with the same definition of "random sinusoidal wave" simultaneously appear, i.e., $\text{disturbance} = A_1 \sin 2\pi t / T_1 + A_2 \sin 2\pi t / T_2$. On the other hand, the "combinational sinusoidal wave" adds damped sinusoidal waves defined by $e^{-(t-t_0)/T} A \sin 2\pi (t - t_0) / T$, on all 3 observation elements. The time steps to initiate damped sinusoidal wave t_0 are randomly selected and this disturbance continues till the end of the episode. The "bias" cases with the amplitude 1.0 and the "noise" cases with $\sigma = 1.0$ are also selected in this experiment. The normalized total reward of the episode after 1000 time of trials is illustrated in Fig. 17. The "comb. sin" and "damped sin" represent "combinational sinusoidal wave" and "damped sinusoidal wave" respectively. On the first column, the result of the "random sinusoidal wave" is shown as a reference. The trained network could perform except in "noise" disturbance. The dynamic model of disturbance exists in "combinational sinusoidal wave", "damped sinusoidal wave" and "bias" cases. As discussed in Section 3, the required behavior is different between the "noise" case and the other three cases. This result reinforces the hypothesis that the network trained in "random sinusoidal wave" utilizes the dynamic model of the disturbance and the system dynamic model and is compatible with the environment under the existence of temporally correlated disturbance.

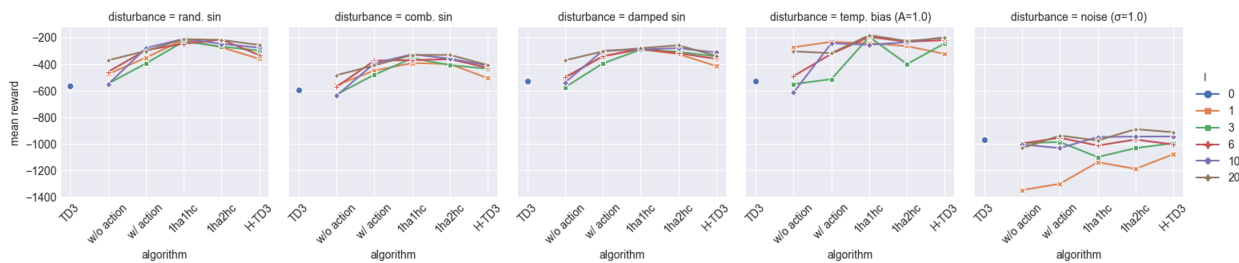


Figure 17: Generalisability

7 Related Work

7.1 Utilizing RNN in RL

There are many existing developments that utilize RNN for RL algorithms to solve POMDP. A few examples are reviewed in this section.

RL-LSTM The utilization of LSTM in RL has been discussed for a long time. In the earlier development, RL-LSTM [29] was presented with a simple grid T-maze experiment using Advantage(λ) learning [30]. In their T-maze experiment, the agent is required to remember the first observation in the entire episode to reach the goal with optimal action. It was shown that RL-LSTM could effectively perform in this non-Markovian scenario. In the recent context of RL, the deep neural network is coupled with the gated recurrent neural network to address the challenge of solving POMDP.

Deep Recurrent Q-learning (DRQL) In Deep Recurrent Q-learning (DRQL) [6], LSTM cells were added to the network by replacing the first dense layer after a convolutional network of DQN [31] in discrete action space. In their work, two types of updates were considered; Bootstrapped Sequential Updates and Bootstrapped Random Updates. The former randomly selects episodes and selected full episodes are replayed from the first step to the end. Hence, the hidden state of LSTM is carried out without initialization throughout one episode. The latter case randomly selects the point of the episode and unrolls the experience for certain time steps. Bootstrapped Sequential Updates can capture longer sequential information but it violates the random sampling policy of DQN. Bootstrapped Random Updates can keep the random sampling but captures the information in a shorter time scale since it requires hidden states of LSTM to be initialized at the beginning of each step. Both types showed similar performance in their investigation, and Bootstrapped Random Updates was finally applied for further discussion because it takes a shorter time to train. In their work, the past action information was not considered, instead, integrated visual information from the console screen is received as input.

Recurrent DPG (RDPG) Heess et al. [28] developed Recurrent DPG (RDPG) by extending DPG [32] with LSTM in actor-critic style by defining actor and critic as $\mu^\theta(h_t)$ and $Q^\mu(h_t, a_t)$ in terms of observation-action history

$h_t = (o_1, a_1, o_2, a_2, \dots, o_{t-1}, a_{t-1}, o_t)$. $\mu^\theta(h_t)$ describes a deterministic policy μ with parameters θ . LSTM is used to summarise the history to make it scalable in POMDP. Similar to Bootstrapped Sequential Updates in DRQL, during the update, a minibatch of N episodes is sampled to construct histories h_t^i ($i = 1 \dots N$), and the target values are computed for each sampled episode through BPTT. It was tested in several environments but the most related ones are "the under-actuated pendulum" and "cartpole swing up" examples. In the experiments, the velocity-related information was removed from the observation. RDPG could learn the tasks which DDPG could not perform.

7.2 Separating between estimation and control

It is also a common approach to separate the estimation and control strategy using information state in reinforcement learning for POMDP condition [33, 34]. The information states are updated based on Bayesian inference. Then, the control strategies are learned by taking the information state. Unlike our discussed methods, this approach explicitly generates the information state and policy takes estimated states. It supports the idea to consider past action information and also processes the sequence up to current information in the same stream as discussed in Section 5.

8 Conclusion

In this paper, the TD3 algorithm has been extended with the LSTM network to solve POMDP. When the disturbance is dynamically changing, it is beneficial to have a policy that dynamically adapts to the new environments. In this context, the inclusion of only observation sequences is not sufficient to construct internal state representation. When the policy is separated into estimation and control parts, belief states are generated from the sequence of state and action in POMDP. This framework is implicitly applicable for the end-to-end model-free RL. We have presented that adding an action sequence can improve the robustness of the achieved performance without the separation of the policy into these two components. The structure to treat the sequence was also discussed. The results showed that it is better to process the past sequence and the current information in the same channel. Also, we proposed a new method called H-TD3 which can significantly reduce the computational time by using the representation of the trajectory information encoded in the actor network for initialisation of the critic network.

For our future work, the generalizability should be further investigated. It was understood that the trained role of the network would differ depending on the characteristics of the disturbances. Developing an algorithm which covers both types of disturbances would take the RL application closer to real-world implementation.

Acknowledgments

This work is partially funded by QuadSAT. We would like to thank them for their support.

A Appendix

A.1 Network structure

Table 3: Structure

Algorithm	Actor network	Critic network
LSTM-TD3	Lin(obs dim+act dim, 128), Lin(obs dim, 128) ReLU, ReLU LSTM(128,128), N/A Lin(256,128) ReLU Lin(128,1) tanh	Lin(obs dim+act dim, 128), Lin(obs dim+act dim, 128) ReLU, ReLU LSTM(128,128), N/A Lin(256,128) ReLU Lin(128,1)
LSTM-TD3 _{1ha1hc}	Lin(obs dim+act dim, 128) ReLU LSTM(128,128) Lin(128,128) ReLU Lin(128,1) tanh	Lin(obs dim+act dim, 128) ReLU LSTM(128,128) Lin(128,128) ReLU Lin(128,1)
LSTM-TD3 _{1ha2hc}	Lin(obs dim+act dim, 128) ReLU LSTM(128,128) Lin(128,128) ReLU Lin(128,1) tanh	Lin(obs dim+act dim, 128), Lin(act dim, 128) ReLU, ReLU LSTM(128,128), N/A Lin(256,128) ReLU Lin(128,1)
H-TD3	Lin(obs dim+act dim, 128) ReLU LSTM(128,128) Lin(128,128) ReLU Lin(128,1) tanh	Lin(obs dim+act dim, 128) ReLU LSTM(128,128) Lin(128,128) ReLU Lin(128,1)
TD3	Lin(obs dim, 128) ReLU Lin(128,128) ReLU Lin(128,1) tanh	Lin(obs dim+act dim, 128) ReLU Lin(128,128) ReLU Lin(128,1)

Lin: linear layer

A.2 The number of parameters

Table 4: The parameter of numbers (obs dim= 3, act dim= 1)

Algorithm	The number of parameters (actor, critic)
LSTM-TD3	166273, 166401
LSTM-TD3 _{1ha1hc}	149377, 149377
LSTM-TD3 _{1ha2hc}	149377, 166017
H-TD3	149377, 149377
TD3	17153, 17281

References

- [1] OpenAI Gym. <https://gymnasium.farama.org/>. Accessed: 2023-01-14.
- [2] Hanna Kurniawati. Partially observable markov decision processes (pomdps) and robotics. *arXiv preprint arXiv:2107.07599*, 2021.
- [3] Pablo Hernandez-Leal, Bilal Kartal, and Matthew E Taylor. A survey and critique of multiagent deep reinforcement learning. *Autonomous Agents and Multi-Agent Systems*, 33(6):750–797, 2019.
- [4] Takahiro Miki, Joonho Lee, Jemin Hwangbo, Lorenz Wellhausen, Vladlen Koltun, and Marco Hutter. Learning robust perceptive locomotion for quadrupedal robots in the wild. *Science Robotics*, 7(62):eabk2822, 2022.
- [5] Xiujun Li, Lihong Li, Jianfeng Gao, Xiaodong He, Jianshu Chen, Li Deng, and Ji He. Recurrent reinforcement learning: a hybrid approach. *arXiv preprint arXiv:1509.03044*, 2015.
- [6] Matthew Hausknecht and Peter Stone. Deep recurrent q-learning for partially observable mdps. In *2015 aaai fall symposium series*, 2015.
- [7] Abhik Singla, Sindhu Padakandla, and Shalabh Bhatnagar. Memory-based deep reinforcement learning for obstacle avoidance in uav with limited environment knowledge. *IEEE Transactions on Intelligent Transportation Systems*, 22(1):107–118, 2019.
- [8] Michael Janner, Qiyang Li, and Sergey Levine. Offline reinforcement learning as one big sequence modeling problem. *Advances in neural information processing systems*, 34:1273–1286, 2021.
- [9] Lili Chen, Kevin Lu, Aravind Rajeswaran, Kimin Lee, Aditya Grover, Misha Laskin, Pieter Abbeel, Aravind Srinivas, and Igor Mordatch. Decision transformer: Reinforcement learning via sequence modeling. *Advances in neural information processing systems*, 34:15084–15097, 2021.
- [10] Ramin Hasani, Mathias Lechner, Alexander Amini, Daniela Rus, and Radu Grosu. Liquid time-constant networks. In *Proceedings of the AAAI Conference on Artificial Intelligence*, volume 35, pages 7657–7666, 2021.
- [11] Bokui Shen, Fei Xia, Chengshu Li, Roberto Martín-Martín, Linxi Fan, Guanzhi Wang, Claudia Pérez-D’Arpino, Shyamal Buch, Sanjana Srivastava, Lyne Tchapmi, et al. igibson 1.0: A simulation environment for interactive tasks in large realistic scenes. In *2021 IEEE/RSJ International Conference on Intelligent Robots and Systems (IROS)*, pages 7520–7527. IEEE, 2021.
- [12] C Daniel Freeman, Erik Frey, Anton Raichuk, Sertan Girgin, Igor Mordatch, and Olivier Bachem. Brax—a differentiable physics engine for large scale rigid body simulation. *arXiv preprint arXiv:2106.13281*, 2021.
- [13] Joanne Truong, Max Rudolph, Naoki Yokoyama, Sonia Chernova, Dhruv Batra, and Akshara Rai. Rethinking sim2real: Lower fidelity simulation leads to higher sim2real transfer in navigation. *arXiv preprint arXiv:2207.10821*, 2022.
- [14] Richard S Sutton and Andrew G Barto. *Reinforcement learning: An introduction*. MIT press, 2018.
- [15] Sudharsan Ravichandiran. *Hands-On Deep Learning Algorithms with Python: Master deep learning algorithms with extensive math by implementing them using TensorFlow*. Packt Publishing Ltd, 2019.
- [16] Sepp Hochreiter and Jürgen Schmidhuber. Long short-term memory. *Neural computation*, 9(8):1735–1780, 1997.
- [17] Junyoung Chung, Caglar Gulcehre, Kyunghyun Cho, and Yoshua Bengio. Gated feedback recurrent neural networks. In *International conference on machine learning*, pages 2067–2075. PMLR, 2015.
- [18] Scott Fujimoto, Herke Hoof, and David Meger. Addressing function approximation error in actor-critic methods. In *International conference on machine learning*, pages 1587–1596. PMLR, 2018.
- [19] Timothy P Lillicrap, Jonathan J Hunt, Alexander Pritzel, Nicolas Heess, Tom Erez, Yuval Tassa, David Silver, and Daan Wierstra. Continuous control with deep reinforcement learning. *arXiv preprint arXiv:1509.02971*, 2015.
- [20] Hado Hasselt. Double q-learning. *Advances in neural information processing systems*, 23, 2010.
- [21] Lingheng Meng, Rob Gorbet, and Dana Kulić. Memory-based deep reinforcement learning for pomdps. In *2021 IEEE/RSJ International Conference on Intelligent Robots and Systems (IROS)*, pages 5619–5626. IEEE, 2021.
- [22] Judea Pearl et al. Models, reasoning and inference. *Cambridge, UK: CambridgeUniversityPress*, 19(2), 2000.
- [23] Dimitri Bertsekas. *Dynamic programming and optimal control: Volume I*, volume 1. Athena scientific, 2012.
- [24] Milos Hauskrecht. *Planning and control in stochastic domains with imperfect information*. PhD thesis, Massachusetts Institute of Technology, 1997.

- [25] Milos Hauskrecht. Value-function approximations for partially observable markov decision processes. *Journal of artificial intelligence research*, 13:33–94, 2000.
- [26] Brian Gaudet and Richard Linares. Adaptive guidance with reinforcement meta-learning. *arXiv preprint arXiv:1901.04473*, 2019.
- [27] Volodymyr Mnih, Adria Puigdomenech Badia, Mehdi Mirza, Alex Graves, Timothy Lillicrap, Tim Harley, David Silver, and Koray Kavukcuoglu. Asynchronous methods for deep reinforcement learning. In *International conference on machine learning*, pages 1928–1937. PMLR, 2016.
- [28] Nicolas Heess, Jonathan J Hunt, Timothy P Lillicrap, and David Silver. Memory-based control with recurrent neural networks. *arXiv preprint arXiv:1512.04455*, 2015.
- [29] Bram Bakker. Reinforcement learning with long short-term memory. *Advances in neural information processing systems*, 14, 2001.
- [30] Mance E Harmon and Leemon C Baird III. Multi-player residual advantage learning with general function approximation.
- [31] Volodymyr Mnih, Koray Kavukcuoglu, David Silver, Andrei A Rusu, Joel Veness, Marc G Bellemare, Alex Graves, Martin Riedmiller, Andreas K Fidjeland, Georg Ostrovski, et al. Human-level control through deep reinforcement learning. *nature*, 518(7540):529–533, 2015.
- [32] David Silver, Guy Lever, Nicolas Heess, Thomas Degris, Daan Wierstra, and Martin Riedmiller. Deterministic policy gradient algorithms. In *International conference on machine learning*, pages 387–395. PMLR, 2014.
- [33] Andreas A Malikopoulos. On separation between learning and control in partially observed markov decision processes. *arXiv preprint arXiv:2211.14972*, 2022.
- [34] Maxime Gasse, Damien Grasset, Guillaume Gaudron, and Pierre-Yves Oudeyer. Causal reinforcement learning using observational and interventional data. *arXiv preprint arXiv:2106.14421*, 2021.